Tetrahedron Vol. 44, No 3, pp. 925 to 940, 1988
Printed in Great Britain

0040-4020/88 $3.00+ 00
Pergamon Journals Ltd

DIVERSITY OF THE GRAMICIDIN A SPATIAL STRUCTURE: TWO-DIMENSIONAL ^{1}H NMR STUDY IN SOLUTION

V.F.Bystrov and A.S.Arseniev

Shemyakin Institute of Bioorganic Chemistry, USSR Academy of Sciences
Ul. Miklukho-Maklaya, 16/10, Moscow V-437, USSR

(*Received in USA 7 July* 1987)

Abstract: Theoretical consideration reveals a unique relationship between NMR spectral parameters and possible types of the gramididin A spatial structure. By means of two dimensional NMR spectroscopy four distinct species were detected simultaneously in ethanol solution. Comparison of experimental data and theoretical conclusions demonstrates that species 1 and 2 are left-handed parallel double helices $\uparrow\uparrow\P\P^{5}_{LD}{}_{6}$ differing in relative arrangement of the two polypeptide chains within the dimers, species 3 is left-handed antiparallel double helix $\uparrow\downarrow\P\P^{5}_{LD}{}_{6}$, and species 4 is a mirror image of species 1, i.e. right-handed parallel double helix $\uparrow\uparrow\P\P^{5}_{LD}{}_{6}$. The results are compared with those on spatial structures of the peptide in complex with cesium (right-handed antiparallel double helix $\uparrow\downarrow\P\P^{7}_{LD}{}_{2}$) and of the gramicidin A transmembrane ion-channel (N-terminal to N-terminal single-stranded dimer $\uparrow^{6.3}_{ID}\uparrow^{6.3}_{LD}$).

Gramicidin A (GA) is a linear pentadecapeptide,
HCO-L-Val^1-Gly^2-L-Ala^3-D-Leu^4-L-Ala^5-D-Val^6-L-Val^7-D-Val^8-L-Trp^9-D-Leu^{10}-L-Trp^{11}-D-Leu^{12}-L-Trp^{13}-D-Leu^{14}-L-Trp^{15}-NHCH$_2$CH$_2$OH,
produced by *Bacillus brevis* during transition from vegetative phase to sporulation of the bacteria. Its biological activity has been attributed to inhibition of transcription by RNA polymerase[1]. The antibacterial activity of GA is stipulated by its ability to increase the membrane permeability to monovalent cations[2].

It was shown[3] that biological and antibacterial activities of GA are independent and, in principle, could be mediated by different spatial structures of the peptide. Two specific types of GA spatial structures (fig. 1), namely, single-stranded dimers[4] and double-stranded helices[5] were proposed from molecular modelling and extensively characterized by conformational energy calculations[6]. It was also demostrated, that GA has distinct spatial structures in different artificial milieus: (i) four conformation species were traced in nonpolar organic solvents[5]; (ii) presumably one of those species, as well as the complex GA with cesium were crystallized[7] and (iii) GA incorporated into phosphatidylcholine vesicles[8] or liposomes[9], and lysolecithin[10] or SDS[11] micelles adopts very specific structure attributed to the channel state of the peptide.

Some evidences in favour of definite conformational structures of GA in different environments were provided both from spectroscopic[8,10,12] and from functional

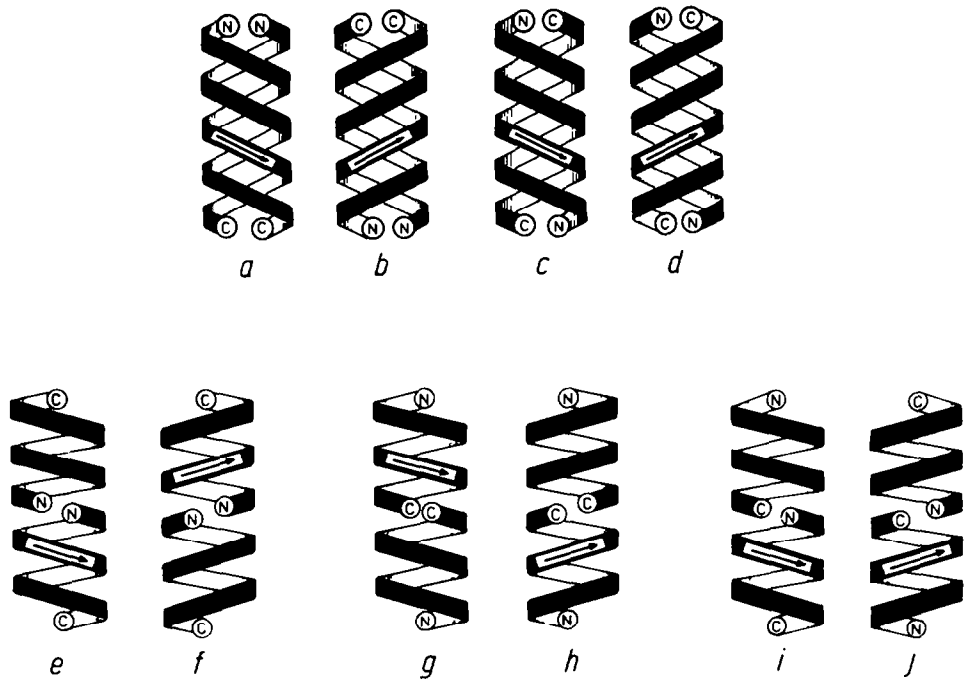

Figure 1. Schematic presentation of the backbone folding of dimeric gramicidin A structures. Double stranded helices: (*a*) and (*b*) left-and right-handed $\uparrow\uparrow\pi\pi_{LD}$, (*c*) and (*d*) left- and right-right handed $\uparrow\downarrow\pi\pi_{LD}$. Single-stranded helices: (*e*) and (*f*) left- and right-handed head-to-head dimers $\overrightarrow{\pi}_{LD}\overleftarrow{\pi}_{LD}$, (*g*) and (*h*) left- and right-handed tail-to-tail dimers $\overleftarrow{\pi}_{LD}\overrightarrow{\pi}_{LD}$, (*i*) and (*j*) left- and right-handed head-to-tail dimers $\overrightarrow{\pi}_{LD}\overrightarrow{\pi}_{LD}$. Arrow marks one of the two backbone chains oriented from left to right towards C-terminal in figure 2.

measurments[13] of modified GA analogues. Nonetheless the proposed spatial structures were not validated untill recent studies by two-dimensional (2D) NMR spectroscopy.

Herein we describe our results on 2D NMR conformational analysis of GA conformational species in nonpolar organic solvent. With regain to previous findings the special attention is given to relationships between features of an environment and promoted spatial structure of the peptide.

RESULTS AND DISCUSSION

Short-range proton-proton distances are unique features of distinct GA spatial structures. Confidence in a spatial structure reconstructed from NMR spectral data is governed by two key factors: (i) single-valued correspondence between NMR data and spatial structure and (ii) adequate agreement between theoretically expected NMR parameters and those experimentally measured. With this in mind let us show that NMR spectroscopy provides a unique solution for spatial structure of every single-stranded or double-stranded GA dimer.

Different types of double- and single-stranded dimers of GA are schemed in fig. 1. The basis of any dimer is β-structure - parallel or/and antiparallel. Thanks to the alternation of *L*- and *D*- amino acid residues in the GA sequence, the side chains of all residues are located on one side of the β-sheet structure. As a

result the β-sheet might be rolled into helix, where side chains form the lipophilic external surface and backbone peptide groups provide the relative separate hydrophilic space.

NMR spectroscopy provides three types of information on a polypeptide spatial structure: spin-spin couplings of the H-NC$^{\alpha}$-H and H-C$^{\alpha}$C$^{\beta}$-H protons, solvent accessibilities of the individual amide groups, and nuclear Overhauser effects (NOE) between spatially close protons.

Spin-spin couplings of H-NC$^{\alpha}$-H protons are useful in determining the different types of secondary structure (α-helices, β-sheets, etc.)[14] rather than in distinguishing GA dimers (fig. 1), all of which have the coupling constant in the 7-10 Hz region. Solvent accessibilities of the amide groups are of utility to the general characterisation of spatial structures, but it was used only as a complementary information because of lack of the straightforward connection with fine details of conformation. Thus identification of GA dimers is based primarily on NOE's data which manifest the shortrange proton-proton distances and hence the mutual arrangement of the amino acid residues in space.

To clarify the mutual arrangement of the amino acid residues in GA helical dimers, their developments on the plane were drawn (fig. 2). Fig. 2 demonstrates the distinct helical dimers specified by two parameters: n and m. Parameter n correlates with the number of residues per helical turn and its sign specifies handedness of a helix (table 1 and 2). The minimum value of $|n|=4$ corresponds to 5.6 residues per turn for double helices or 4.4 residues per turn for single-stranded helices. These helices have a smallest diameter of internal hydrophilic cavity. The other sorts of double helices could have 7.2 ($|n|=6$), 9.0 ($|n|=8$) or 10.8 ($|n|=10$) residues per turn, while single-stranded helices could have 6.3 ($|n|=6$) residues per turn. The parameter m reflects a displacement of two polypeptide chains as depicted in fig. 2.

The spatially close amino acid residues of GA dimers give rise to different patterns of short-range proton-proton distances depending on whether the dimer is formed by parallel or antiparallel double helices or by terminal-to-terminal linked single-stranded helical structures. The short-range distances are specified in fig. 3 and tabulated in tables 1 and 2 for different types of GA dimers. The distances assigned to dpecific protons of amino acid residues provide exhaustive discription of spatial structure of the GA helical dimers. To identify distinct types of helices and their parameters n and m, it is useful to assemble characteristic maps of short-range proton-proton distances. These connectivity maps for different double and single-stranded helical dimers are shown in fig. 4.

Gramicidin A in nonpolar organic solvents. More than 10 years ago Veatch et al.[5a] detected four slowly interconverting dimeric GA species in nonpolar organic solvents (methanol, ethanol, ethylacetate and dioxane). By means of infrared spectroscopy the species were tentatively assigned to antiparallel (species 3) and parallel (species 1,2 and 4) double helices[5a]. A more recent 2D NMR study of isolated species 3 confirmed the Veatch's assignment and revealed its detailed spatial structure as left-handed double helix $\uparrow\uparrow\pi\pi^{5}_{LD}.^{6}$ with 5.6 residues per turn[15]. Besides it was shown[16] that the shortened alalog of GA, des |L-Ala^{3}, D-Leu^{4}, L-Ala^{5}, D-Val^{6}|-gramicidin A, is right-handed double helix $\uparrow\uparrow\pi\pi^{5}_{LD}.^{6}$ with 5.6 residues per turn. Circular dichroism and infrared spectra of the analog are very much like those of species 4.

To get a further insight into the GA spatial structure in nonpolar organic solvent, the equilibrated mixture of GA species in ethanol solutions was studied by means of 2D NMR spectroscopy. The solvent was chosen because of the high dimerisation constant [5b] and high solubility of GA in the etanol. Fingerprint of the

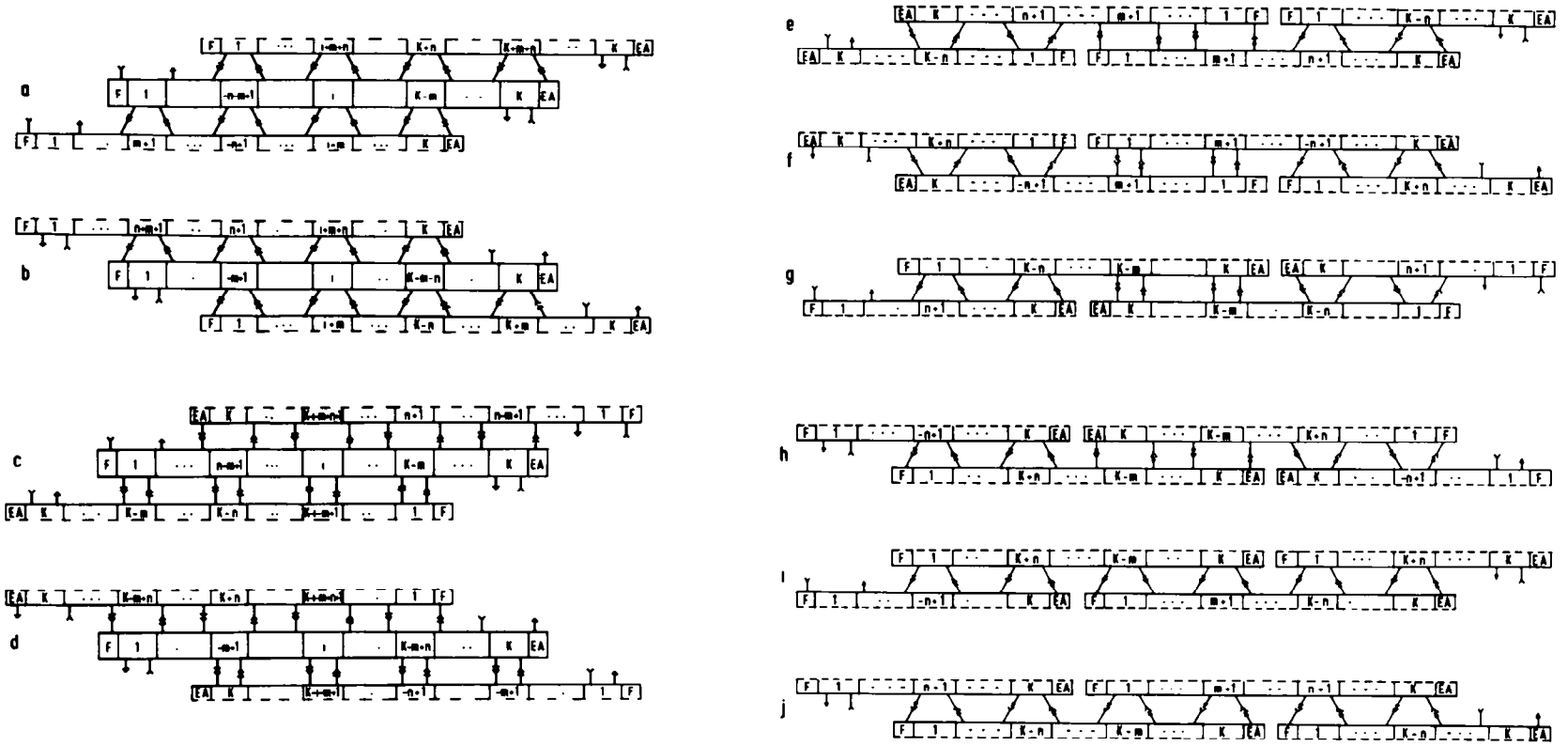

Figure 2. Developments of gramicidin A dimeric structures which are lettered as in figure 1. The helices were cut along the shaded lines and unrolled. Amino acid numbers are inside of rectangles, F - N-terminal formyl proup, EA - ethanol amine moiety. The hydrogen bonding patterns are shown by arrows (NH-groups) and by reverse arrows (CO-groups). In the figure and subsequent discussion the used parameters are: K - number of amino acid residues in polypeptide chain (for GA K=15), n - parameter which defines handedness and number of residues per helical turn and m reflects the displacement of two chains in case of double helical dimer (a-d) or degree of junction of two single-stranded helices (e-j).

Table 1. Short-range proton-proton distances in double helices

Type of helix and helical parameters[a]	i = L-Residue		i = D-Residue	
	Notation[b]	Range[c], Å	Notation[b]	Range[c], Å
↑↓ left-handed	$d_{N\alpha}^{i,q}$	2.7-3.0	$d_{N\alpha}^{i,p}$	2.4-3.0
$n < -4$	$d_{\alpha N}^{i,p}$	2.7-3.0	$d_{\alpha N}^{i,q}$	2.4-3.0
$q = i+m$	$d_{NN}^{i,q+1}$	3.7-4.0	$d_{NN}^{i,p-1}$	3.7-4.0
$p = q+n$	$d_{\alpha\alpha}^{i,p+1}$	3.7-4.8	$d_{\alpha\alpha}^{i,q-1}$	3.7-4.8
↑↑ right-handed	$d_{N\alpha}^{i,q}$	2.4-3.0	$d_{N\alpha}^{i,p}$	2.7-3.0
$n > 4$	$d_{\alpha N}^{i,p}$	2.4-3.0	$d_{\alpha N}^{i,q}$	2.7-3.0
$q = i+m$	$d_{NN}^{i,q+1}$	3.7-4.0	$d_{NN}^{i,p-1}$	3.7-4.0
$p = q+n$	$d_{\alpha\alpha}^{i,p+1}$	3.7-4.8	$d_{\alpha\alpha}^{i,q-1}$	3.7-4.8
↑↓ left-handed	$d_{N\alpha}^{i,q+1}$	2.6-3.2	$d_{N\alpha}^{i,p+1}$	3.3-3.2
$n > 4$	$d_{NN}^{i,q}$	3.4-3.3	$d_{NN}^{i,p}$	3.4-3.3
$q = K-i-m+1$	$d_{\alpha N}^{i,p+1}$	3.3-3.2	$d_{\alpha N}^{i,1+1}$	2.6-2.0
$p = q+n$	$d_{\alpha\alpha}^{i,p}$	2.3-2.3	$d_{\alpha\alpha}^{i,q}$	2.0-2.3
↑↓ right-handed	$d_{N\alpha}^{i,q+1}$	3.3-3.2	$d_{N\alpha}^{i,p+1}$	2.6-3.2
$n < -4$	$d_{NN}^{i,q}$	3.4-3.3	$d_{NN}^{i,p}$	3.4-3.3
$q = K-i-m+1$	$d_{\alpha N}^{i,p+1}$	2.6-3.2	$d_{\alpha N}^{i,q+1}$	3.3-3.2
$p = q+n$	$d_{\alpha\alpha}^{i,p}$	2.0-2.3	$d_{\alpha\alpha}^{i,q}$	2.3-2.3

[a] ↑↑ and ↑↓ denote parallel and antiparallel arrangement of strands in double helices. For definition of helical parameters n, m and K see figures 2-4 and text; [b] Distance notations as in figure 3; [c] The first distance corresponds to the double helix with smallest number of residues per turn ($|n|=4$) and the second distance corresponds to the non-twisted β-sheet structures (unrolled double helix).

Table 2. Short-range proton-proton distances in single-stranded helices

Type of helix and helical parameters[a]	i = L-Residue		i = D-Residue	
	Notation[b]	Range[c], Å	Notation[b]	Range[c], Å
left-handed	$d_{N\alpha}^{i,q}$	2.8-3.0	$d_{N\alpha}^{i,p}$	2.5-3.0
$n > 4$	$d_{\alpha N}^{i,p}$	2.8-3.0	$d_{\alpha N}^{i,q}$	2.5-3.0
$q = i+n$	$d_{NN}^{i,q+1}$	3.6-4.0	$d_{NN}^{i,p-1}$	3.6-4.0
$p = i-n$	$d_{\alpha\alpha}^{i,p+1}$	3.6-4.8	$d_{\alpha\alpha}^{i,q-1}$	3.6-4.8
right-handed	$d_{N\alpha}^{i,q}$	2.5-3.0	$d_{N\alpha}^{i,p}$	2.8-3.0
$n < -4$	$d_{\alpha N}^{i,p}$	2.5-3.0	$d_{\alpha N}^{i,q}$	2.8-3.0
$q = i+n$	$d_{NN}^{i,q+1}$	3.6-4.0	$d_{NN}^{i,p-1}$	3.6-4.0
$p = i-n$	$d_{\alpha\alpha}^{i,p+1}$	3.6-4.8	$d_{\alpha\alpha}^{i,q-1}$	3.6-4.8

a, b and c as in table 1.

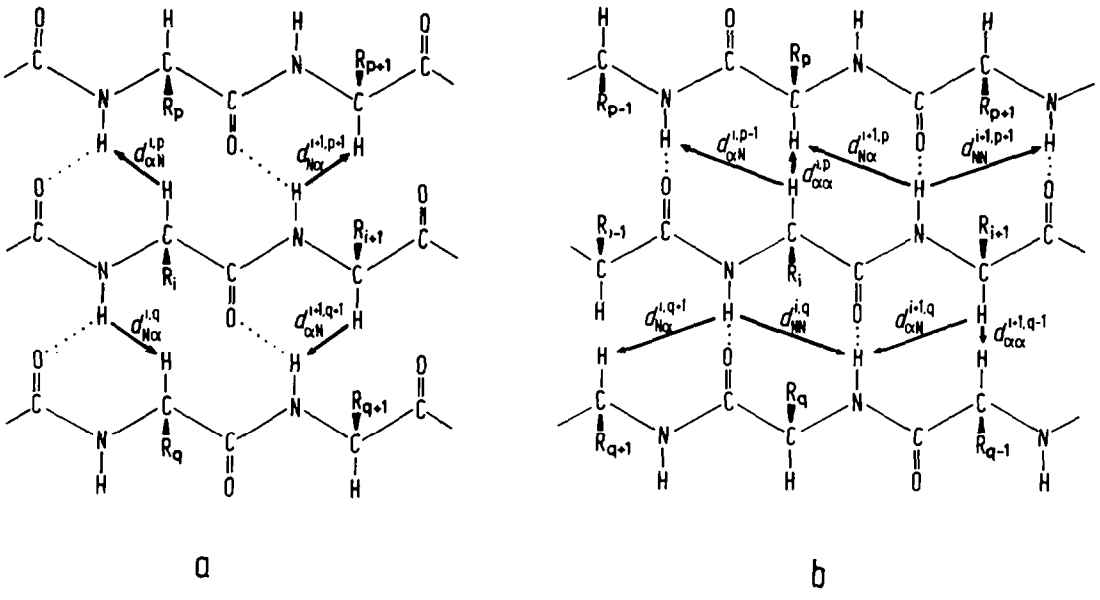

Figure 3. Standard parallel (a) and antiparallel (b) β-sheets. Sidechains R of amino acid residues are located above the figure plane. Residues *i*, *p* and *q* have *L*-configuration and adjancent residues have *D*-configuration. Hydrogen bonds are shown by dots. The arrows indicate short-range proton-proton distances *d*. Subscripts *N* and *α* denote NH and $C^{\alpha}H$ protons, respectively, and superscripts indicate the residues that give the short-range distances.

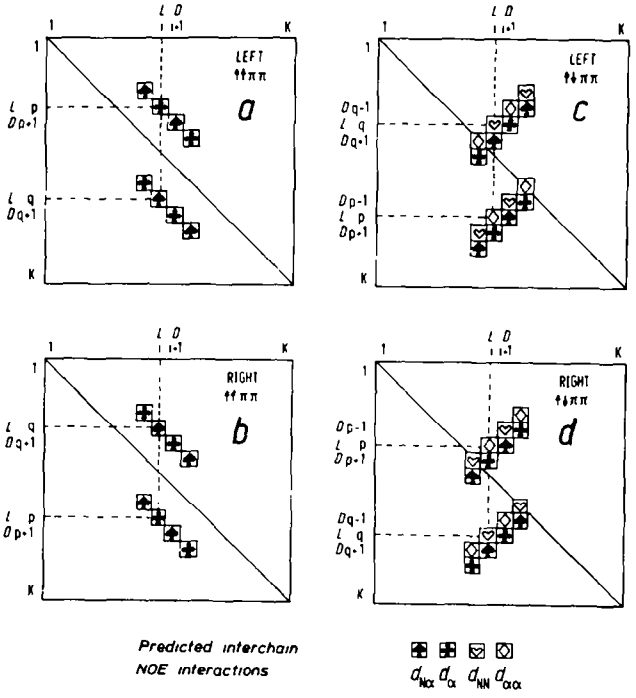

Figure 4.

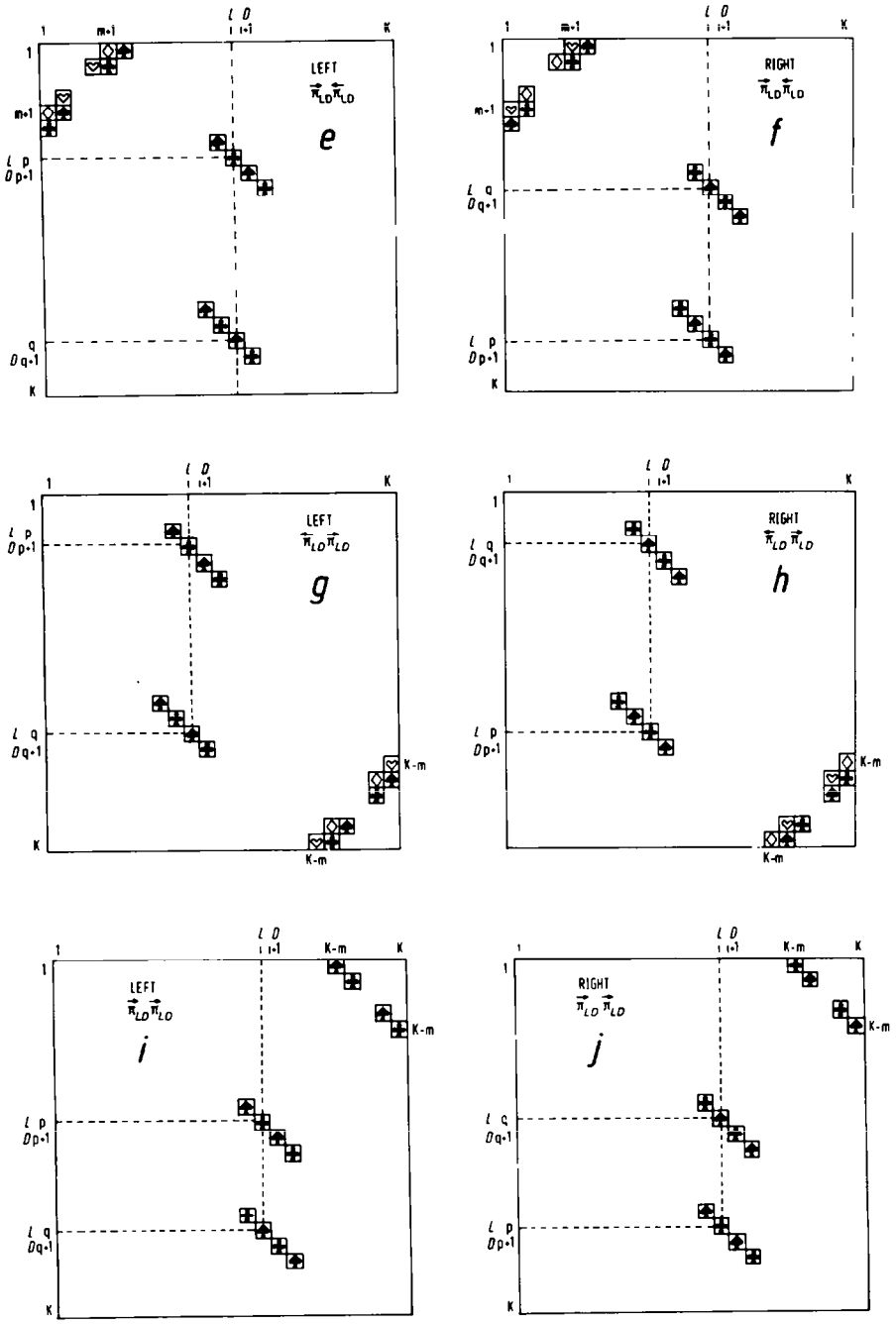

Lgure 4. (Continued) Characteristic maps of the short-range (<4 Å) proton-proton lstances of gramicidin A dimeric species *a-j* depicted in figures 1 and 2. The ces of the maps are marked with the amino acid sequence of two polypeptide chains. etters L and D denote the chirality of the residues. Notations of the short-range coton-proton distances are specified at the bottom. First and second subscripts orrespond to residues numbered on the abscissa and ordinate of the maps, respectively.

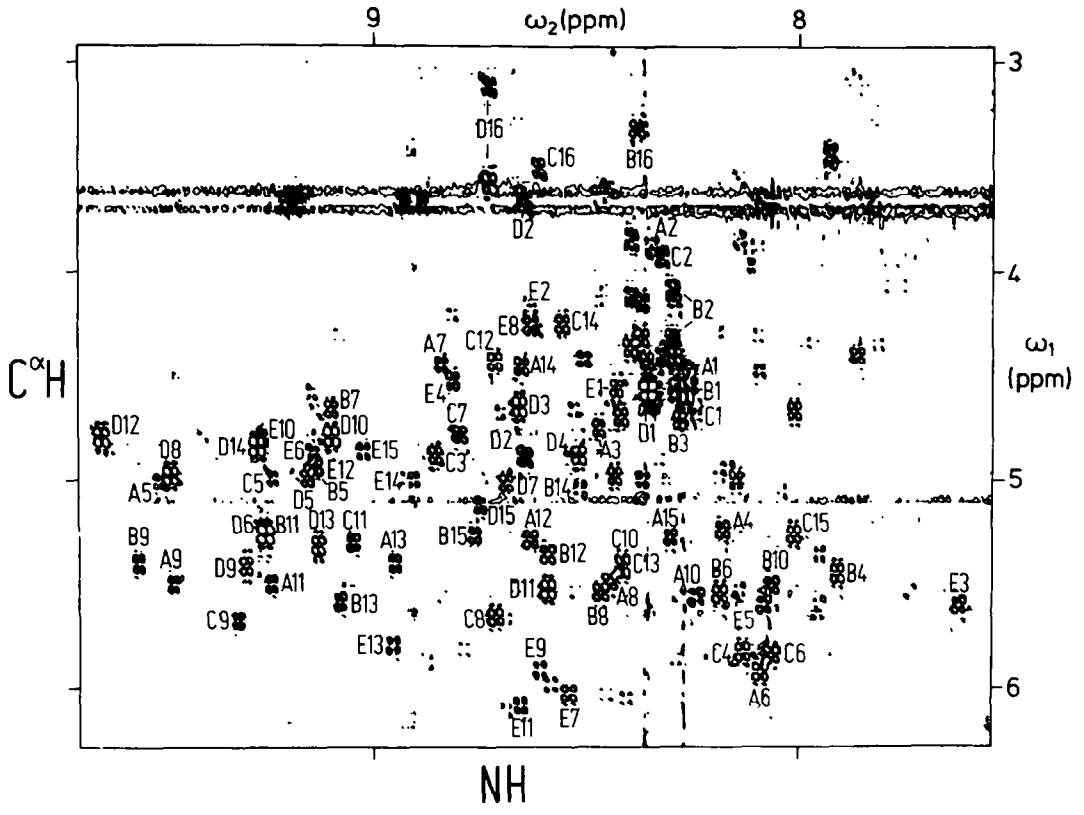

Figure 5. Fingerprint region of a 500 MHz phase-sensitive absorption mode double quantum filtered COSY spectrum of a 30 mM gramicidin A in CD_3CD_2OH at 30°. The cross-peaks of NH/$C^{\alpha}H$ protons are identified by letters A (species 1), B and C (two unsymmetrical polypeptide chains of species 2), D (species 3) and E (species 4) and by numbers corresponded to the amino acid residue position in the gramicidin A primary structure.

NH/$C^{\alpha}H$ region of GA COSY spectrum in CD_3CD_2OH solution is shown in fig. 5. The spectrum contains over 100 NH/$C^{\alpha}H$ cross-peaks, which correspond to at least five distinct conformational species in equilibrium.

Proton signals were assigned to specific position in the amino acid sequence of GA in two steps. The spin systems of amino acid residues (alanines, glycines, valines, leucines and tryptophanes) were identified by analysis of the COSY and in sophisticated cases by analysis of the homonuclear Hartman-Hahn crosspolarization spectra (e.g. see fig. 6) at 30, 40, 50 and 60°C. Different temperatures were used to clarify ambiguous assignments of the NH resonances, which could overlap at certain temperature, but are shifted differently when temperature is changed.

The next step was the assignment of a spin system to specific position of the amino acid residue in the primary structure of GA. This was done by sequential resonance assignment in the NOESY spectra through $^1d_{\alpha N}$, $^1d_{NN}$ and $^1d_{\beta N}$ NOE-connectivities of the amide $N_{i+1}H$ proton of i+1 residue with the $C_i^{\alpha}H$, N_iH and C_i^{β} protons of the preceding i residue, respectively, as proposed in [18]. Again different temperatures were used in order to clarify ambiguous assignments. The sequential resonance assignments were based primarily on $^1d_{\alpha N}$ connectivities and in some cases were complemented by $^1d_{\beta N}$ connectivities. The $^1d_{NN}$ connectivities always were absent.

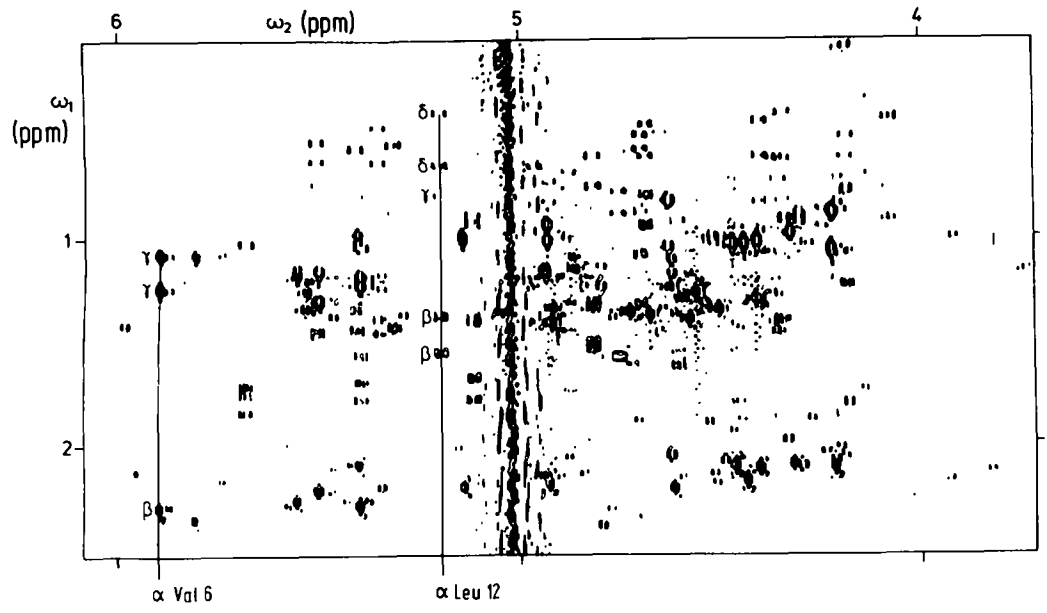

Figure 6. Spectral region ω_1 = 0.1-2.5 ppm and ω_2 = 3.7-6.1 ppm of a 500 MHz phase-sensitive absorption mode homonuclear Hartman-Hahn cross-polarization spectrum (mixing time 40 ms) of a 30 mM gramicidin A in CD_3CD_2OD at 50°C. The region contains abundant set of cross-peaks for $C^{\alpha}H/C^{\beta}$ and $C^{\alpha}H/C^{\gamma}H_3$ protons of valine residues as well as for $C^{\alpha}H/C^{\beta}H$, $C^{\alpha}H/C^{\gamma}H$ and $C^{\alpha}H/C^{\delta}H_3$ of leucine residues. For illustration cross-peaks $C^{\alpha}H/C^{\beta}H$ and $C^{\alpha}H/C^{\gamma}H_3$ of D-Val^6 and cross-peaks $C^{\alpha}H/C^{\beta}H$, $C^{\alpha}H/C^{\gamma}H$ and $C^{\alpha}H/C^{\delta}H_3$ of D-Leu^{12} are indicated for polypeptide chain A (species 1).

As a result all the signals of five conformational species of the GA polypeptide chain were assigned. The $NH/C^{\alpha}H$ cross-peaks of each amino acid residue of the species are marked in COSY spectrum (fig. 5) by letters A-E corresponded to different conformational states of the molecule and by numbers related to the position in the GA amino acid sequence. The presence of $^1d_{\alpha N}$-connectivities as well as magnitudes of spin-spin coupling constants of the $H\text{-}NC^{\alpha}\text{-}H$ protons (7-10 Hz) suggests that polypeptide chains A-E have extended conformations. In addition to $^1d_{\alpha N}$ connectivities, the NOESY spectra of GA in ethanol solution (e.g. fig. 7) contain many NOE connectivities between nonadjacent amino acid residues in the GA sequence and even between residues of two nonequivalent (B and C) polypeptide chains. The data are summarized in fig. 8 a-d in the form of connectivity maps.

The maps of NOE connectivities manifest the short-range proton-proton distances and hence they are directly comparable with theoretically devised maps of short-range proton-proton distances (fig. 4). The comparison leads us to identification of species 1-4 conformations in ethanol solution as pointed out in caption to figure 8 a-d. A schematic drawing of the species is presented in figure 8 a-d, respectively. Species 1,2 and 4 are the parallel and species 3 is the antiparallel double helices with 5.6 residues per turn. Species 3 was also found for GA crystallized from ethanol and subsequently dissolved in dioxane with minimum interconversion protocol[11]. Species 1,3 and 4 have C_2 symmetry axes with result that chemicaly

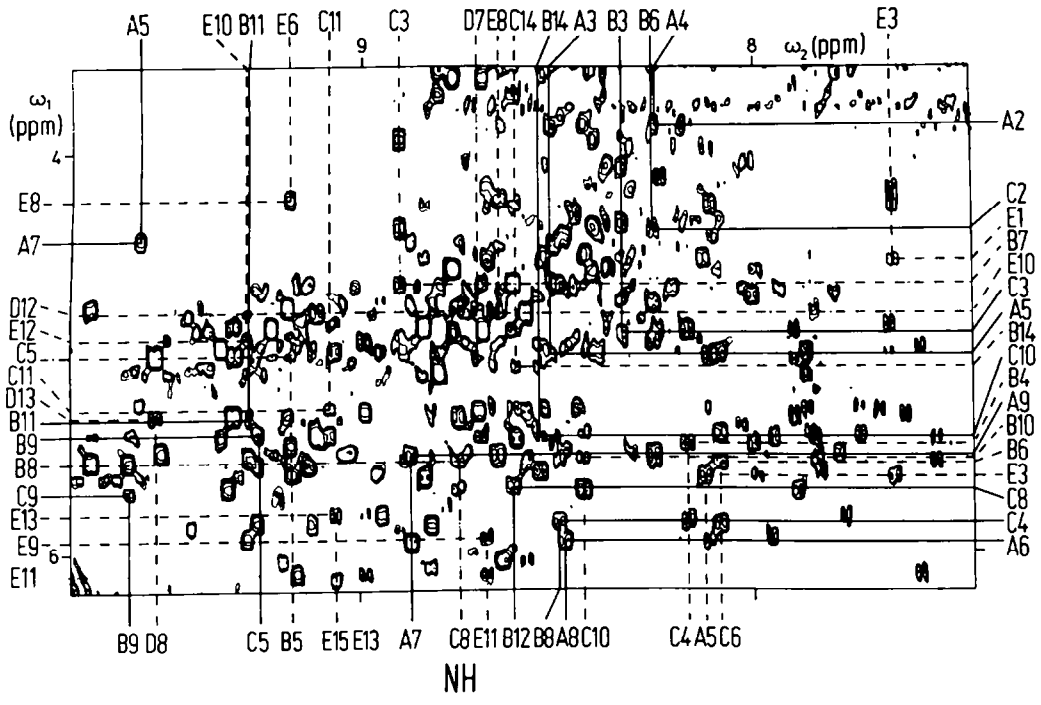

Figure 7. Spectral region ω_1= 3.6-6.2 ppm, ω_2= 7.6-9.7 ppm of a 500 MHz phase-sensitive absorption mode NOESY spectrum (mixing time 200 ms) of a 30 mM gramicidin A in CD_3CD_2OH at 30°C. The amide NH proton chemical shifts are indicated by the assignments at the top and bottom of the contour map while those of $C^{\alpha}H$ protons on the left- and right-hand sides of the plot. The used notations are as in figure 5.

equivalent protons of two polypeptide chains of a dimer have identical chemical shifts. Backbone folding of species 4 is a mirror image of species 1 as manifested by interrepositioning of $d_{\alpha N}^{ij}$ and $d_{N\alpha}^{ij}$ short-range proton-proton distances (see fig. 8a and d). It is noteworthly that handedness of species 4 is opposite to that of species 1,2 and 3, which correlate with signs of CD curves of the species[5a].

Thus the 2D NMR spectroscopy reveals the detailed backbone folding of four GA species detected by Veatch et al [5]. All the four are double helices with 5.6 residues per turn and have the maximum number of hydrogen bonds (28) allowable for GA dimers. The number is equal to $2(K+1)-|n|$ and realized at the specific relations between parameters n and m[19].

Hence one of the main factors stabilizing formation of the double helices in nonpolar organic solvents, is the maximum number of internal hydrogen bonds, although of ten GA double helices with 28 hydrogen bonds[19] only four are found in ethanol solution. It is likely that another factor which limits the number of GA species in nonpolar organic solvent is specific interaction between side chains on the surface of double helices. This is in line with observation that the GA analog with modified amino acid sequence in dioxane solution gives only one dominant species - right-handed double helix $\uparrow\uparrow\pi\pi^{5,6}_{LD}$ [16]. In addition, only one of four GA species, namely, species 3 is crystallized from ethanol solution [5a,15], presumably, because this species is favored by interactions between surfaces of GA dimers.

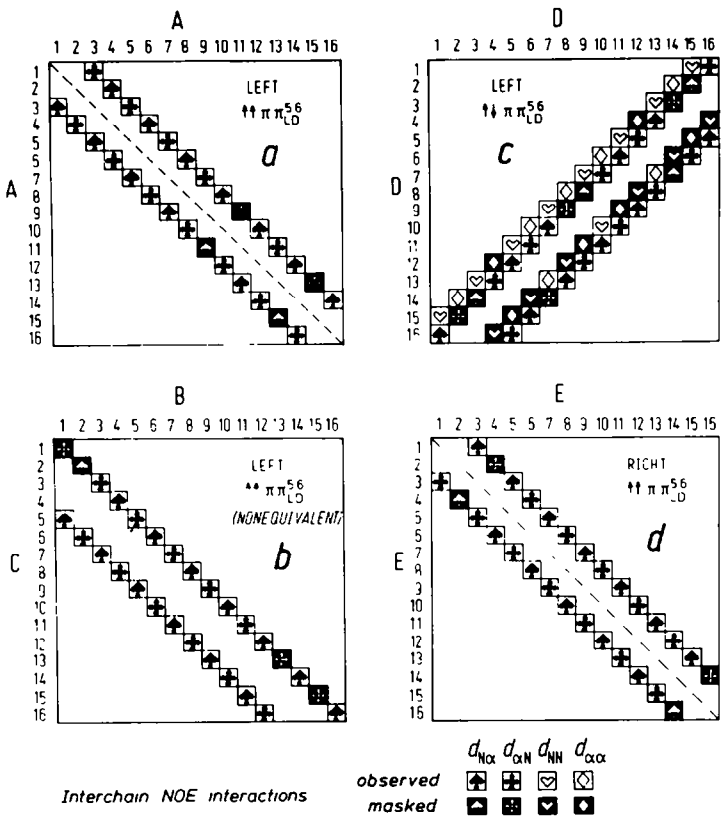

Figure 8. Maps of NOE-connectivities between backbone NH and $C^{\alpha}H$ protons of four gramicidin A dimeric species detected in ethanol solution. The maps correspond to: (*a*) left-handed double helix $\uparrow\uparrow\pi\pi^{5}_{LD}{}_{\bullet}{}^{6}$, n = -4, m = 2 (species 1); (*b*) left-handed double helix $\uparrow\uparrow\pi\pi^{5}_{LD}{}_{\bullet}{}^{6}$, n = -4, m = 4 (species 2 with two unequivalent chains B and C); (*c*) left-handed double helix $\uparrow\downarrow\pi\pi^{5}_{LD}{}_{\bullet}{}^{6}$, n = 4, m = 0 (species 3); and (*d*) right-handed double helix $\uparrow\uparrow\pi\pi^{5}_{LD}{}_{\bullet}{}^{6}$, n = 4, m = -2 (species 4). Notations of the NOE-connectivities are specified at the bottom of the figure.

Other gramicidin A structures. The spatial structure of GA in different milieus has been the focus of considerable studies. We shall give short account of these structures.

The binding of GA to monovalent cations was studied in methanol-chloroform (1:1) composite solvent, ideally suitable for preparation of the stable complex[20] in high concentration. GA dissolved in the solvent forms a mixture of four double helical species described in the previous section. An addition of cesium thiocyanide to the solution leads to one predominant species - right-handed antiparallel double helix $\uparrow\downarrow\pi\pi^{7}{}_{\bullet}{}^{2}$ (n=-6, m=0) with 7.2 residues per turn, as revealed by means of 2D NMR techniques[20]. The same right-handed double helix $\uparrow\downarrow\pi\pi^{7}_{LD}{}^{2}$ is a predominant conformation for GA complexes with KCNS and TlCNS, although a fraction of the species was found somewhat lower than in case of the cesium complex. The antiparallel aligmenent of two GA polypeptide chains provides two symmetrical and thereby iden-

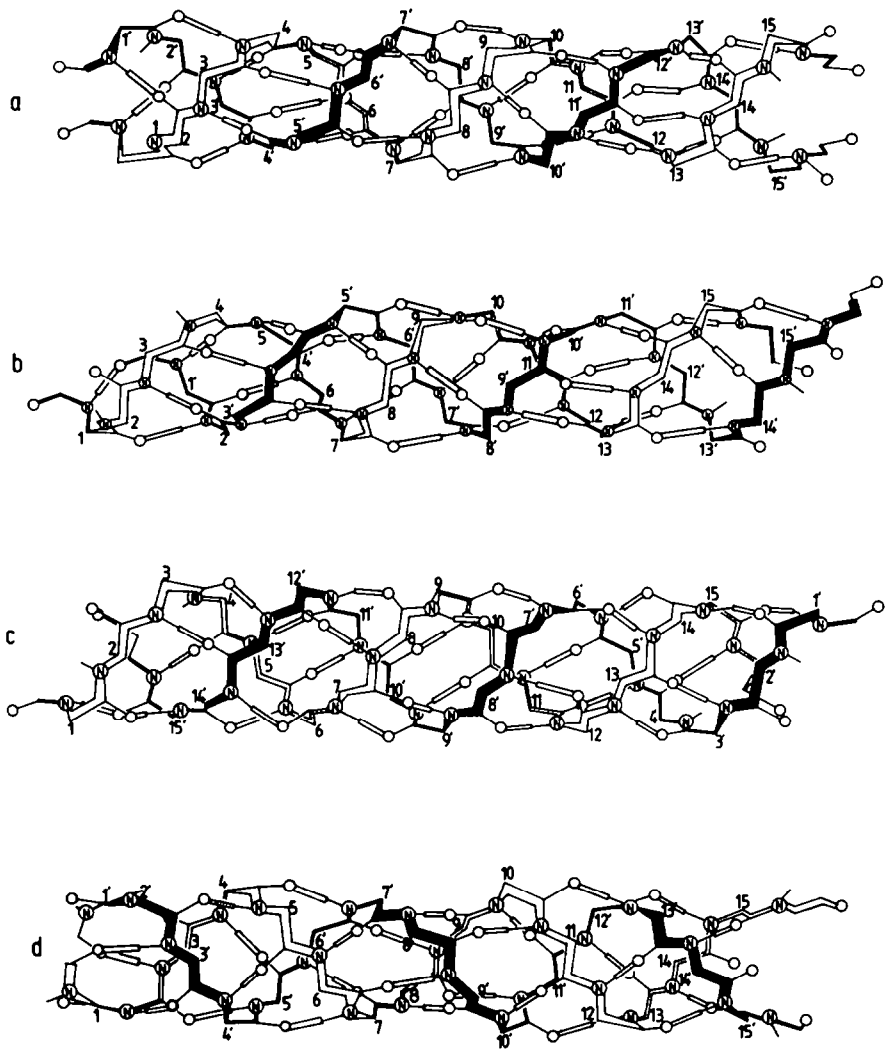

Figure 9. Schematic presentation of the gramicidin A double helices detected in ethanol solution by 2D NMR spectroscopy: (*a*) species 1, (*b*) species 2, (*c*) species 3 and (*d*) species 4. Side chains of amino acid residues are omitted for clarity. Hydrogen bonds are shown by emply bars. The short-range proton-proton distances of the species 1-4 correspond to NOE-connectivity maps shown in figure 8 *a-d*, respectively. For sake of completetness spatial structures of (*e*) gramicidin A complex with cesium[20] and (*f*) gramicidin A transmembrane ion-channel[11] are also presented.

tical binding sites for polarizable monovalent cations potassium, thallium and, particularly, cesium whose diameters fit the size of the lipophilic axial cavity of the double helix. Contrary, ions with smaller diameters, such as lithium and sodium, induce random coil conformation of the peptide sistead of double helices originally spesented in chloroform-methanol solution[21]. Thus lithium and sodium thiocyanides operate like hydrogen bond smashers and together with chloroform-me-

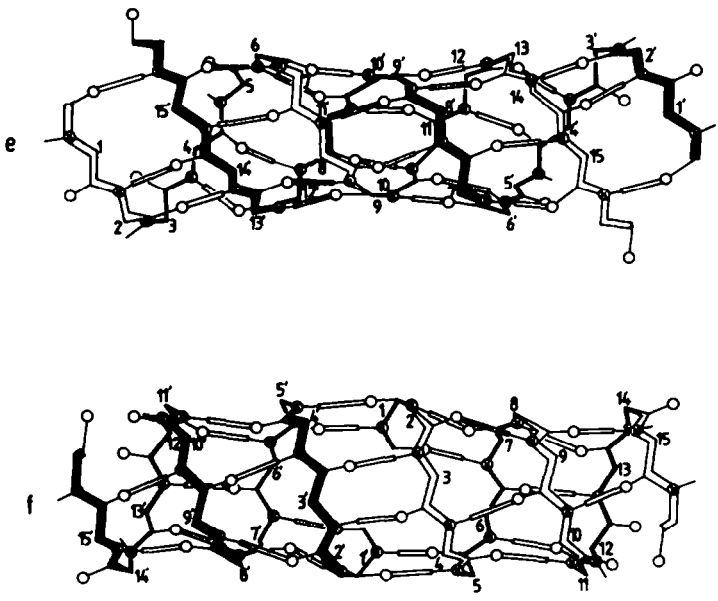

Figure 9. (Continued)

thanol provide lipophilic environment for side chains and hydrophilic surrounding for backbone of GA. The similar effect on GA spatial structure was observed in dimethyl sulfoxide[22], where no ordered conformations were detected.

An ultimate target of many GA studies was a spatial structure of GA ion-channel in bilayer membranes. It was widely accepted, that GA ion-channel structure is left-handed $\overrightarrow{\pi}^{6.3}_{LD}\overleftarrow{\pi}^{6.3}_{LD}$ helical dimer proposed by Urry[4]. Several lines of evidence were used to prove the model, among them: (i) effect of chemical modification on GA mediated ion-conductunce[13,23]; (ii) NMR measurments of accessibility of N- and C-terminal GA labels to either aqueous or lipophilic paramagnetic probes[8]; (iii) IR and Raman spectra in the amide I region [12a]; (iv) fluorescence energy transfer between fatty acid probes and tryptophans of GA[12b]; and (v) ion-induced carbonyl ^{13}C chemical shifts of selectively ^{13}C-enriched GA[10]. All the evidences are consistent with N-terminal to N-terminal dimer formed by two single-stranded helices. In addition the (v) data were used to determine the helix sense and location of ion-binding sites[10].

On the other hand, GA spatial structure in SDS-micelles, as shown recently by 2D NMR spectroscopy[11], is right-handed $\overrightarrow{\pi}^{6.3}_{LD}\overleftarrow{\pi}^{6.3}_{LD}$ helical dimer. Noteworthy, CD spectrum[24] of GA in SDS-micelles[11a,b] coincides with those found previously in different membrane like milieus (vesicles[9c], liposomes[9a,b] and lysolecithin micelles[10]) and attributed[10] to ion-channel state of the peptide. Thus the dilemma arises: CD spectra of right-handed and left-handed $\overrightarrow{\pi}^{6.3}_{LD}\overleftarrow{\pi}^{6.3}_{LD}$ helices are identical or ion-induced carbonyl carbon chemical shifts of GA in lysolecithin have to be reinterpreted. We would like to point out that, first, the data on ion-induced chemical shifts for carbonyl carbons of L-amino acid residues (Val^1, Ala^3, Ala^5, Val^7, Trp^9, Trp^{11}, Trp^{13} and Trp^{15}) are consistent both with right-handed and

left-handed $^{+6.3}_{\pi_{LD}}{}^{+6.3}_{\pi_{LD}}$ helices[10b]. Second, in case of D-amino acid residues ion-induced carbonyl carbon chemical shifts were measured for only two residues, namely D-Val[8] and D-Leu[14] [10]. The same two measurments were used for the conclusion on the left-handed sense on the $^{+6.3}_{\pi_{LD}}{}^{+6.3}_{\pi_{LD}}$ helix[10]: (i) the absence of ion-induced carbonyl carbon chemical shift for D-Val[8] was considered as an indication that its carbonyl is well removed from the cation binding site and (ii) ion-induced chemical shift for the D-Leu[14] carbonyl was treated as its nearness to the same cation binding site formed by the carbonyl groups of tryptophan residues, although the opposite sign of the ion-induced chemical shift of D-Leu[14] as compared with those of L-Trp residues is still unexplained.

In contrast to Urry et al.[10], we suppose that the data for D-amino acid residues do not contradict the right-handed sense of the $^{+6.3}_{\pi_{LD}}{}^{+6.3}_{\pi_{LD}}$ helix.

Indeed, since ion-induced chemical shift is a complicated function both of a distance between ion and carbonyl group and of an orientation of the carbonyl bond in respect to the ion[25], the lack of the ion-induced chemical shift is well explained by cancelation of different terms. The cancelation will occur most likely if the cation is exactly above the plane of the $^{N}\!\!\diagdown\!\!C^{\alpha}\!\!\diagup\!\!C' = O$ group [25c]. It is the case of the D-Val[8] carbonyl bond in right-handed $^{+6.3}_{\pi_{LD}}{}^{+6.3}_{\pi_{LD}}$ helix[26].

However, carbonyls of L-Trp[9,11,13,15] and D-Val[8] on the one hand, and carbonyl of D-Leu[14] on the other cannot simultaneiosly interact with the cation in case of right-handed helix - the sites are well separated. Thus the GA channel has four cation binding sites, instead of two sites originally assumed[10] at interpretation of ion-induced carbonyl carbon chemical shifts. An examination of molecular model of the right-handed $^{+6.3}_{\pi_{LD}}{}^{+6.3}_{\pi_{LD}}$ helix leads to identification of the four sites: two symmetrical sites (≈20 Å apart) at the channel entrance formed by carbonyl groups of D-Leu[10,12,14] and another two symmetrical sites (≈15 Å apart) at a depth of the channel, where ions are sensed by carbonyl groups of L-Trp[9,11,13,15]. Cations are in fast exchange between the four sites and bulk solvent and not more than two sites might be simultaneously occupied. Thus the right-handed $^{+6.3}_{\pi_{LD}}{}^{+6.3}_{\pi_{LD}}$ helix fits data on ion-induced carbonyl carbon chemical shifts[10]. The above consideration is in line with the three barriers-four sites model of the GA ion transport mechanism advocated by Eisenman and Sandblom[27].

Up to date six distinct stable structures of GA in different milieus are revealed by two dimensional NMR spectroscopy (fig. 9): in nonpolar organic solvents - three parallel and one antiparallel double helices with 5.6 residues per turn; complex with cesium - right-handed antiparallel double helix with 7.2 residues per turn, and in SDS-micelles as well as in liposomes, vesicles, lysolecithyn micelles and bilayer membranes - N-terminal to N-terminal right-handed single-stranded helical dimer with 6.3 residues per turn. Thus GA gives a representative example, when one amino acid sequence codes several different stable conformational structures depending on a milieu. A further variation of milieu properties or modification of the GA amino acid sequence might lead to the discovery of new spatial structures.

EXPERIMENTAL

Gramicidin A was obtained form Gramicidin D (Serva) by countercurrent distribution[28]. CD_3CD_2OD (99% deuterium) and CD_3CD_2OH (98% deuterium) were from Isotope (USSR).

All two-dimensional NMR spectra were recorded in the pure phase absorption mode using the time proportional phase incrementation method[29]. The following spectra were recorded on a Bruker WM 500 spectrometer: double quantum filtered COSY spectra[30], NOESY spectra[31] at mixing time of 200 ms, and homonuclear Hartman-

Hahn crosspolarization (MLEV17 HOHAHA) spectra[32] at mixing time of 40 ms. In the case of the CD_3CD_2OH sample, the OH resonance was suppressed by irradiation during all times except detection period.

Characteristic short-range proton-proton distances for double- and single-stranded helices were calculated by means of CONFORNMR program[11c] where standart ECEPP/2 bond angles and bond lengths[33] and torsion angles[6b] were used.

REFERENCES

1. [a] N. Sarkar, D. Langley and H. Paulus, Biochemistry 18, 4536 (1987); [b] R. Fisher and T. Blumenthal, Proc. Natl. Acad. Sci. USA. 79, 1045 (1982).
2. F. Harold and J. Baarda, J. Bacteriol. 94, 53 (1967).
3. H. Paulus, N. Sarkar, P.K. Mukherjee, D. Langley, V.T. Ivanov, E.N. Shepel and W. Veatch, Biochemistry 18, 4532 (1979).
4. D.W. Urry, Proc. Natl. Acad. Sci. USA 68, 672 (1971).
5. [a] W.R. Veatch, E.T.Fossel and E.R. Blout, Biochemistry 13, 5249 (1974); [b] W.R. Veatch and E.R. Blout, Biochemistry 13, 5257 (1974).
6. [a] G.N. Ramachandran and R. Chandrasekharan, Indian J. Biochem. Biophys.9,1(1972); [b] B. Lotz, F. Colonna-Cesari, F. Heitz and G. Spach, J. Mol. Biol.106, 915 (1976); [c] F. Collona-Cesari, S. Premilat, F. Heitz, G. Spach and B. Lotz, Macromolecules 10, 1284 (1977).
7. [a] R.E. Koeppe II, K.O. Hodgson and L. Stryer, J. Mol. Biol. 121, 41 (1978); [b] R.E. Koeppe II and B.P.Schoenborn, Biophys.J. 45, 503 (1984); [c] B.A. Wallace, Biophys. J. 49, 295 (1986).
8. [a] S. Weinstein, B.A. Wallace, J.S. Morrow and W.R. Veatch, J. Mol. Biol. 143, 1 (1980); [b] S. Weinstein, J.T. Durkin, W.R. Veatch and E.R. Blout, Biochemistry 24, 4374 (1985).
9. [a] L.Masotti, A. Spisni and D. Urry, Cell Biophys. 2, 241 (1980); [b] S.V. Sychev and V.T. Ivanov, Biol. Membrany (USSR) 1, 1109 (1984); [c] B.A. Wallace, W.R. Veatch and E.R. Blout, Biochemistry 20, 5754 (1981).
10. [a] For reviews, see: D.W. Urry, T.L. Trapane and R.U. Prasad, Science 221, 1064 (1983); [b] D.W. Urry, J.T. Walker and T.L. Trapane, J. Membrane Biol. 69,225(1982).
11. [a] A.S. Arseniev, I.L. Barsukov, V.F. Bystrov, A.L. Lomize and Yu.A. Ovchinnikov, FEBS Lett. 1986, 168 (1985); [b] A.S. Arseniev, I.L. Barsukov, V.F. Bystrov and Yu.A. Ovchinnikov, Biol. Membrany (USSR) 3, 437 (1986); [c] A.S. Arseniev, A.L. Lomize, I.L. Barsukov and V.F. Bystrov, Biol. Membrany (USSR) 3, 1077(1986).
12. [a] V.M. Naik and S. Krimm, Biophys. J. 49, 1147 (1986); [b] L.T. Boni, A.J. Connoly and A.M. Kleinfeld, Biophys. J. 49, 122 (1986).
13. For review see: E. Bamberg, H.-J. Apell, H. Alpes, E. Gross, J.L. Morell, J.F. Hrbaugh, K. Janko and P. Lauger, Federation Proc. 37, 2633 (978).
14. [a] A.S. Arseniev, V.I. Kondakov, V.N. Maiorov, T.M. Volkova, E.V. Grishin, V.F. Bystrov and Yu.A. Ovchinnikov, Bioorgan, Khim. (USSR) 9,(1983); [b] A. Pardi, M. Billiter and K. Wütrich, J. Mol. Biol. 180, 741 (1984); [c] G. Wagner, D. Neuhaus, E. Worgotter, M. Vasak. J.H.R. Kagi and K. Wüthrich, J. Mol. Biol. 187, 131 (1986).
15. [a] A.S. Arseniev, V.F. Bystrov, V.T. Ivanov and Yu.A. Ovchinnikov, FEBS Lett. 165, 51 (1984); [b] A.S. Arseniev, I.L. Barsukov, S.V. Sychev, V.F. Bystrov, V.T. Ivanov and Yu.A. Ovchinnikov, Biol. Membrany (USSR) 1, 5 (1984).
16. A.S. Arseniev, I.L. Barsukov, E.N. Shepel, V.F. Bystrov and V.T. Ivanov, Bioorgan, Khim. (USSR) 11, 5 (1985).
17. S.V. Sychev, N.A. Nevskaya, St. Jrdanov, E.N. Shepel, A.I. Miroshnikov and V.T. Ivanov, Bioorgan. Kim. (USSR) 9, 121 (1980).

18. K. Wüthrich, G. Wieder, G. Wagner and W. Braun, J. Mol. Biol. 155, 311 (1982).
19. I.L. Barsukov, A.S. Arseniev and V.F. Bystrov, Bioorgan. Khim. (USSR) 13, in press (1987).
20. A.S. Arseniev, I.L. Barsukov and V.F. Bystrov, FEBS. Lett. 180, 33 (1985).
21. V.F. Bystrov, A.S. Arseniev, I.L. Barsukov, A.L. Lomize, Bulletin Magn. Reson. 8, 84 (1987).
22. F. Heitz, A. Heitz and Y. Trudelle, Biophys. Chem. 24, 149 (1986).
23. [a] For reviews, see: J.T. Durkin, Philosophy Doctor Thesis, Harward University (1986); [b] O.S. Andersen, Ann. Rev. Physiol. 46, 531 (1984).
24. Right- and left-handed GA double helices are readily recognized by CD spectra, see above and ref. 5a.
25. [a] A.D. Bickingham, Can. J. Chem. 38, 300 (1960); [b] W.J. Horsley and H. Sternlicht, J. Amer. Chem. Soc. 90, 3738 (1968); [c] V.F. Bystrov, S.L. Portnova, T.A. Balashova, S.A. Kozmin, Yu.D. Gavrilov and V.A. Afanas'ev, Pure and Applied Chem. 36, 19 (1973).
26. See figure 7 in D.W. Urry, T.L. Trapane, S. Romanowski, R.J. Bradley and K.U. Prasad, Int. J.Peptide Protein Res. 21, 16 (1983).
27. [a] G. Eisenman and J.P. Sandblom, Physical Chemistry of Transmembrane Ion Motions (Edited by G. Spach), pp. 329-348, Elsevier Science Publishers B.V., Amsterdam (1983); [b] G. Eisenman and J.P. Sandblom, Biophys. J. 45, 88 (1984).
28. L.R. Ramachandran, Biochemistry 2, 1138 (1963).
29. D. Marion and K. Wüthrich, Biochem. Biophys. Res. Commun. 113, 967 (1983).
30. M. Rance, O.W. Sørensen, G. Bodenhausen, G. Wagner, R.R. Ernst and K. Wüthrich, Biochem. Biophys. Res. Commun. 117, 479 (1983).
31. J. Jeener, G.H. Meier, P. Bachmann and R.R. Ernst, J. Chem. Phys. 71,4546(1979).
32. A. Bax and D.G. Davis, J. Magn. Reson. 65, 355 (1985).
33. [a] F.A. Momany, R. McGuire, A.W. Burgess and H.A. Scheraga, J. Phys. Chem. 79, 2361 (1975); [b] G. Nemethy, M.S. Pottle and H.A.Scheraga, J. Phys. Chem. 87, 1883 (1983).